

## **Fluoroaromatic Substituents Attached to Carbon Nanotubes Help to Increase Oxygen Concentration on Biocathode in Biosensors and Biofuel Cells**

Maciej Karaskiewicz<sup>a</sup>, Jan F. Biernat<sup>b</sup>, Jerzy Rogalski<sup>c</sup>, Kenneth P. Roberts<sup>d</sup>, Renata Bilewicz<sup>a\*</sup>

<sup>a</sup> *Faculty of Chemistry, University of Warsaw, Pasteura 1, 02-093 Warsaw, Poland,*

<sup>b</sup> *Department of Chemical Technology, Gdansk University of Technology Narutowicza 11/12; 80-233 Gdańsk, Poland*

<sup>c</sup> *Department of Biochemistry, Maria Curie Skłodowska University, Akademicka 19, 20-031 Lublin, Poland*

<sup>d</sup> *Department of Chemistry and Biochemistry, The University of Tulsa, 800 S. Tucker Dr., Tulsa, OK 74104, USA*

### **Abstract**

Based on the known ability of perfluorodecalin/perfluorohydrocarbons to enhance oxygen solubility we modified oxygen sensitive biocathode by adding perfluorinated components to the catholite. This procedure improved the efficiency of the oxygen sensitive cathodes. Glassy carbon electrodes covered with single-wall carbon nanotubes (SWCNTs) with covalently bonded perfluoroaromatic groups were shown to be more sensitive to oxygen, and higher catalytic reduction currents were observed using laccase modified biocathodes allowing to improve the performance of bioelectrodes for fuel cells and oxygen monitoring devices. Maximum current and power density was found for the glucose/oxygen fuel cell composed of anode modified with side-aminoethylated SWCNTs conjugated with glucose dehydrogenase and cathode covered with side-perfluorophenylated SWCNTs and laccase. The open circuit

potential of this cell is  $0.57\pm 0.05$  V and the maximum power density is  $0.865\pm 0.090$  mW/cm<sup>2</sup>. In case of applications of biofuel cells in the biological media, in order to avoid addition of NAD<sup>+</sup> to the solution, we propose binding this cofactor to the aminoethylated SWCNTs. For applications of this biofuel cell in biological media, we propose binding NAD<sup>+</sup> cofactor to the aminoethylated SWCNTs instead of its addition to the electrolyte. The power output  $0.226\pm 0.031$  mW/cm<sup>2</sup> of such cell is somewhat smaller but still satisfactory, and the open circuit potential is  $0.65\pm 0.08$  V.

*Key-words:* arylated carbon nanotubes, perfluoroarylated carbon nanotubes, bioelectrocatalysis, oxygen reduction, glucose oxidation, biofuel cell, laccase.

\*Renata Bilewicz

Faculty of Chemistry, University of Warsaw

ul. Pasteura 1, 02093 Warsaw, POLAND

e-mail: [bilewicz@chem.uw.edu.pl](mailto:bilewicz@chem.uw.edu.pl), tel: +48 22 8220211, fax: +48 22 8225996.

## 1. Introduction

In recent years there has been substantial progress in designing enzyme covered electrodes for enzymatic biofuel cells and biobatteries. These devices that generate energy from readily-available fuels, e.g. sugars or alcohols, attract much attention since they are cheap, work at room temperature and at pH close to physiological, and use enzymes catalyzing oxygen reduction and glucose oxidation. Catalyzed oxygen reduction could proceed directly to water without any harmful intermediates or side products [1-11]. The enzymes are also specific, so no additional membranes separating the cathodic and anodic compartments are needed when the biocathode is used in the enzymatic biofuel cell [4,10-12]. Recently, several promising glucose – oxygen biofuel cells and biobatteries have been reported; increased stability and significantly improved power output have been demonstrated using carbon fiber, carbon nanotubes, carbon black and other nanostructured carbonaceous electrode matrices [13-22]. The effect of oxygen concentration on the biocathode performance was studied both numerically and experimentally [23,24]. As oxygen solubility in aqueous solutions is rather low, improvement of oxygen transport into the enzyme matrix and maintaining its stable concentration at the electrode surface should remove one of the constraints in the application of oxygen based electrodes [25]. During work of the biocathode in the fuel cell, rapid decrease of oxygen concentration in the vicinity of the electrode surface is observed. Thus low concentration of oxygen and its fast depletion at the biocathode are problems to be tackled in order to achieve the stage of practical applications. To solve these issues flow systems, gas-diffusion cathodes and pressed-air-breathing biocathodes have been proposed [26-28].

In the present study, we made use of the ability of perfluorocarbons, to accumulate large quantity of oxygen. This behavior we studied using as an example perfluorodecalin film

placed on the electrode surface. To improve oxygen accumulation on the electrode surface we also designed and synthesized fluoroarylated carbon nanotubes. In our recent papers [29-36] we demonstrated that arylated carbon nanotubes provide efficient pathways for the transfer of electrons between the active center of laccase and the conducting support. The 3-dimensional nanotubes network of modified carbon nanotubes on the electrode is able to accommodate and accumulate huge amount of catalyst [37-40] The phenyl, naphthyl or terphenyl groups bonded to the nanotubes allow stable and durable adsorption of the enzyme and increase the amount of enzyme molecules in suitable orientation to easy exchange electrons with the electrode.

Formerly we presented the synthesis, purification and characterization of arylated SWCNTs [35]. In the present paper we describe the synthesis of SWCNTs equipped with perfluoroaryl residues. These materials retain the laccase binding feature to the arylated carbon nanotubes, and at the same time increase the amount of oxygen concentration close to the electrode surface as it was observed for perfluorodecalin.

At the anode of the biofuel cell, glucose dehydrogenase (GDH) enzyme is used since it does not react directly with oxygen as opposed to glucose oxidase. In the latter case, the performance of anode is decreased because oxygen from the cathode accesses the anodic part and competes with the enzyme; moreover, the  $H_2O_2$  produced in this case destabilizes the enzyme [41,42]. Nicotinamide adenine dinucleotide dependent glucose dehydrogenase (GDH) was chosen; however binding of its  $NAD^+$  cofactor is relatively weak, and therefore it should be either added to the solution, the matrix on the electrode, or immobilized directly together with the enzyme onto the electrode surface [43,44]. Recently, we have shown the immobilization of  $NAD^+$  jointly with the enzyme in the liquid-crystalline lipid matrix and the application of diaphorase to decrease the overpotential of NADH oxidation [37]. Here we propose binding of  $NAD^+$  onto the carbon nanotubes together with the enzyme as the best way to nanostructure the anode surface in the biological fuel cell.



## 2. Experimental

### 2.1. Materials and chemicals

All reagents were of analytical grade; solutions were prepared using Milli-Q water. SWCNTs were from CheapTubes, Brattleboro, USA (purity>90%); or from Nanocyl, Sambreville, Belgium). Perfluorodecalin, perfluoroaniline and perfluorobenzoic acid were from Sigma–Aldrich, while aniline, benzoyl chloride and analytical grade solvents were from POCh Gliwice, Poland.

Thermogravimetric analyses (TGA/DTA) were conducted using Universal V4.3A TA instrument in argon atmosphere at a heating rate of 10°/min. The derivatization degrees were calculated according to recommendations [43-45], assuming temperature of 600°C as sufficiently high for complete detachment of substituents. The calculated results are collected in Table 1.

FT-IR spectra were registered using Genesis II (Mattson) instrument. Materials were prepared in form of KBr pellets. The characteristic bands for the fluorinated species are given in the synthesis section and include C–F frequencies. The spectra for benzoyl derivatives and anilides do not show expected specific bands of noticeable intensity.

Raman spectra were collected using a Witec confocal Raman microscope system (Ulm, Germany) equipped with a fiber-coupled Melles Griot (Carlsbad, CA) argon ion laser operating at 514.5 nm focused through a 60× objective. Collected light was dispersed through a triple monochromator (600 g/mm, 500 nm blaze) and detected with a thermoelectrically cooled (–60 °C) charge-coupled device. In the sample preparation procedure a small amount of carbon nanotubes in powder form was placed between a microscope slide and a cover slip.

## 2.2 SWCNTs purification and modification procedures

### *Purification of SWNTs*

To remove metallic and carbonaceous impurities, the pristine single walled carbon nanotubes purchased from CheapTubes and Nanocyl, were treated with 4 N HCl. The suspension was maintained at 60°C for 6 h under permanent sonication [46, 47] the solid was collected, exhaustively washed with water and vacuum dried.

### *Syntheses of amides*

The synthetic pathways are shown in Scheme 1.

#### *Side 2-aminoethylated-SWCNTs, material 1*

The nanotubes modified with aminoethyl groups on the side-walls were synthesized according to procedure described by Mugadza and coworkers [48]. Purified SWCNT (600 mg), NaNO<sub>2</sub> (800 mg; 12 mmol) and ethylenediamine (1.2 g, 1.35 ml; 12 mmol) were combined and thoroughly triturated. To this, almost solid material in closed test-tube conc. sulfuric acid (0.52 mL; 10 mmoli) was added, mixed with a glass rod and maintained at 60°C for 1 h. The mixture was diluted with water, the solid filtered of and washed with water to neutrality. Finally, the product was washed with methanol and dried in vacuum. IR: C–F = 2367, 2359 and 2337 cm<sup>-1</sup>.

#### *Benzoylated side aminoethyl-SWCNTs, material 2*

A mixture of 100 mg commercial benzoyl chloride added to a suspension of 50 mg of aminoethyl-SWCNTs **1** and 1 ml pyridine was sonicated for 2 h at 50<sup>0</sup> C and then left overnight. The solid was filtered of, washed exhaustively with methanol, next with methylene chloride and vaccum dried.

Insert Scheme 1.

### *Pentafluorobenzoylated side aminoethyl-SWCNTs, material 3*

A mixture of 50 mg of pentafluorobenzoic acid, 1 ml thionyl chloride and 0.01 ml dry pyridine was maintained for 2 h at 50<sup>0</sup> C and left for 2 days at room temperature. Then 2 ml toluene was added and the volatiles were exhaustively removed under reduced pressure. The residue was dissolved in 1 ml dry pyridine, 50 mg of aminoethylated SWCNTs was added and the mixture was sonicated for 4 h at 50<sup>0</sup>C and then left for 2 days at room temp. The solid was filtered of, washed several times with methanol, finally with methylene chloride and dried under reduced pressure. IR: 3422, 2921, 2851, 2371, 2345, 2323, 1654, 1636, 1559, 1542, 1522, 1457 cm<sup>-1</sup>.

### *SWCNTs with terminal carboxylic groups, material 4*

SWCNTs oxidized by means of a mixture of conc. nitric and sulfuric acid produce carboxylic groups at the ends/defect sites of the nanotubes. Thus 260 mg of purified SWCNTs were treated with 50 ml of 3:1 (v/v) sulfuric acid and nitric acid mixture and maintained at 50°C for 4 h under permanent sonication. The mixture was diluted with water on cooling and left overnight. Then the suspension was centrifuged, the sediment mixed with water, sonicated and centrifuged again. The last procedure was repeated five times. Finally the sediment was mixed with methanol, sonicated, centrifuged and dried under reduced pressure; yield 200 mg, c.f. [49].

### *Terminal chlorocarbonyl carbon nanotubes, SWCNTs-COCl, material 5*



The dried oxidized SWCNTs **4** (200 mg) were treated with an excess of thionyl chloride (4 ml) and the mixture was sonicated and maintained at 60°C for 24 h. After removing excess of SOCl<sub>2</sub> under reduced pressure at 60°C (bath temperature) product **5** was obtained.

*Terminal anilide of oxidized SWCNTs, material 6*

To 50 mg portion of product **5** suspended in 2 ml cold dry pyridine 0.1 ml pure aniline was added. The mixture was sonicated for 4 h at 60°C and then left overnight at room temp. The solid was then separated by filtration, washed with methanol, water and again with methanol and vacuum dried.

*Terminal pentafluoroanilide, material 7*

Was analogously obtained by reaction of chloride **5** with pentafluoroaniline. The work up was identical as in the case of material **6**.

*Terminal aminoethylamide of SWCNTs 8*

Aminoethylamide of SWCNTs was prepared by the known method [46] with minor modifications, c.f. [33].

A portion of nanotubes with terminal –COCl residues **5** (100 mg) was treated with 3 ml of dry pyridine and 1 ml of anhydrous ethylenediamine. The suspension was maintained for 24 h at 50-60°C under permanent sonication and then diluted with water. The solid was separated by centrifugation and thoroughly washed with water and methanol, and finally dried in vacuum.

Yield of **8** 100 mg.

Benzoylation (material **9**) and pentafluorobenzoylation (material **10**) products of material **8** were obtained in analogous manner as were obtained materials **2** and **3**.

IR for material **10**: 3422, 2921, 2851, 2371, 2345, 2323, 1654, 1636, 1560, 1542, 1522, 1457 cm<sup>-1</sup>.

Insert Table 1.





Raman spectroscopy has been shown to be a useful tool in monitoring the chemical modification of SWCNTs for some time due to the unique Raman modes produced in CNTs from confinement of electronic and phonon states [33,50-53]. Although Raman characterizations of SWCNTs can be more or less elaborated, most studies have focused on examination of radial breathing modes (RBM), the one phonon disorder (D) band, the first-order tangential graphite (G) band, and the second order G' band. The first-order RBM modes correspond to in phase displacements of  $sp^2$  carbon atoms in the radial direction. When observable, RBM modes can be indicative of the type of SWCNT (metallic or semiconductor), nanotube size, and the degree of nanotube functionalization, where the latter has been attributed to displacement of the Fermi level from attachment of chemical functionality to the SWCNT side-walls [50]. More commonly, monitoring chemical functionalization of SWCNTs has relied on comparison of intensities of the D, G, and G' Raman modes, i.e.,  $I_D/I_G$ ,  $I_{G'}/I_G$ , and  $I_{G'}/I_D$ . Under first principles, as the degree of functionalization increases, the disorder D band increases relative to the graphite G band. Raman spectroscopy has utilized the intensity ratios of nature of the SWCNT under study. As well, the two-phonon G' is the second harmonic of the disorder D band and can as such be used to further the evidence of functionalization as well as provide insight on the homogeneity of the sample product. Discussed here are the Raman results of the functionalized materials in Table 1 in terms of the relative intensities of D, G, and G' bands.

The 2-aminoethylated-SWCNTs (material **1**) produced very minimal RBM modes which is reflective of the Fermi level distribution from attachment to the SWCNT sidewall. The D, G, and G' bands are centered at  $\sim 1343$ ,  $1582$ , and  $2686\text{ cm}^{-1}$ , respectively, with the G band position and width indicative of semiconductor SWCNTs. The weak  $I_D/I_G$  value of 0.055 is indicative of minimal fragmentation of the overall CNT during functionalization. As well, the relative large  $I_{G'}/I_G$  of 0.409 and the bimodal G' indicates the presence of more than one



type of functionalized semiconductor nanotube product after purification. The  $I_G/I_D$  was the largest of all samples tested and provided further evidence that long-range order of the  $sp^2$  carbons remained largely intact. Similarly, samples **2**, **3**, **4**, and **7** revealed very little RBM modes which suggests functionalization was successful. However, in contrast, the D, G, and G' intensity ratios were very similar and indicated a greater degree of functionalization than observed for material **1**. Moreover, in each the G' mode was not bimodal, indicating a more homogeneous product as compared to material **1**. As shown in Table 1, samples **6**, **9**, and **10** produced a similar degree of functionalization, which was higher than the aforementioned samples. In all cases, minimal RBM modes were revealed and the G' was primarily a single mode, indicating once again that a preferential product was obtained in the final purification. Interestingly, the Raman results for material **8** are very similar to those obtained for material **1** in many ways. Although sample **8** is an end-style attachment of aminoethylamide while **1** is attached to the SWCNT sidewall, both amine derivatives show minimal disruption of the  $sp^2$  carbons as evidenced by the small (identical)  $I_D/I_G$  ratio of 0.055. As well, the  $I_{G'}/I_G$  of 0.409 for material **1** and 0.404 for **8** are nearly identical, indicating a stoichiometrically similar degree of functionalization. Further, the  $I_{G'}/I_D$  are also very similar and relatively large compared to the remaining samples presented here. The slight decrease in the material **8**  $I_{G'}/I_D$  could also be visually observed as having less bimodal distribution of the G' mode. Regardless, in both cases, it can be concluded that only a small degree of functionalization was observed, or the type of functionalization had minimal effect on the integrity of the SWCNT  $sp^2$  hybridized structure as observed by Raman spectroscopy. What is more, it can also be concluded that both material **1** and **8** are each a mixture of more than one product obtained after functionalization and purification.

Insert Figure 1.

Insert Figure 2.



Carbon nanotubes, which lead to the highest catalytic oxygen reduction current, were utilized for the preparation of the cathode. Material 3 shows the highest ability for oxygen accumulation [Fig. 3-C], nevertheless all materials were employed for the biofuel cell Scheme 2. Materials 3, 6, 7 and 10 were chosen for electrochemical studies.

#### *Preparation of SWCNTs bioconjugated with glucose dehydrogenase*

The *Pseudomonas sp.* NAD-dependent glucose dehydrogenase (276 U/mg) was obtained from Sigma (St. Louis, USA); *Cerrena unicolor* laccase was obtained as described earlier [34].

Side wall aminoethylated SWCNTs **1** were applied for covalent glucose dehydrogenase (NAD<sup>+</sup>) immobilization (material A and B) and NAD<sup>+</sup> with glucose dehydrogenase bioconjugate immobilization by following strategies:

Material A: SWCNT-(CH<sub>2</sub>)<sub>2</sub>-NH<sub>2</sub> **1** (15 mg) was sonicated 4 h and activated with glutaraldehyde (pentane-1,5-dial; 5% in 0.1 M phosphate buffer pH 7.0) according to [54] in Eppendorf tube by 8 h rotation in Rotator (Neolab, Heidelberg, Germany) at 10 rpm. Then the samples were centrifuged at 10 000 x g for 8 min, washed with MilliQ water and centrifuged under the same as above conditions. The washing procedure was repeated 3 times. Next, the GDH(NAD<sup>+</sup>) solution (138 U) was added to activated suspension of carbon nanotubes and allowed to react for 12 h under rotation at 10 rpm. The washing conditions of the preparation obtained were as above.

Material B: SWCNT-(CH<sub>2</sub>)<sub>2</sub>-NH<sub>2</sub> **1** (15 mg) was sonicated 4 h and activated with EDC (1-ethyl-3-(3-dimethylaminopropyl) carbodiimide; 5% in 0.1 M acetate buffer pH 5.0) according to [55] in Eppendorf tube by 8 h rotation on Rotator at 10 rpm, then mixed with GDH(NAD<sup>+</sup>) solution (138 U and allowed to react for 12 h under rotation at 10 rpm. Next, the samples

were centrifuged at 10 000 x g for 8 min, washed with MilliQ water and centrifuged as above. The washing procedure was repeated 3 times.

**Material C:** SWCNT-(CH<sub>2</sub>)<sub>2</sub>-NH<sub>2</sub> 1 (15 mg) was sonicated 4 h and activated with epoxy (1,4-butanediol diglycidyl ether (dioxirane); 5% in 0.1 M Britton-Robinson buffer pH 10.0) according to [56] in Eppendorf tube by 8 hrs rotation at 10 rpm. Next, the sample was centrifuged at 10 000 x g for 8 min, washed by MilliQ water and centrifuged as above. The washing procedure was repeated 3 times After the activation of SWCNT-(CH<sub>2</sub>)<sub>2</sub>-NH<sub>2</sub> (15 mg) by diglycidyl ether the NAD<sup>+</sup> solution (5 mg) in 0.1 M Britton-Robinson buffer pH 10.0 was added and rotated for 8 h at 10 rpm.

### **Protein binding to SWCNTs**

The obtained above epoxy activated SWCNTs (epoxy-CNT,) were mixed with glucose (0.1%) for 12 h in 0.1 M Britton-Robinson buffer, pH 10.5 as in [57], centrifuged (10 000 x g; 8 min), washed with MilliQ water and centrifuged again. Next, the obtained matrix (gluco-epoxy-CNT) suspended in 0.1 M Britton-Robinson buffer pH 8.0 was rotated in Rotator at 10 rpm for 12 h with GDH(NAD<sup>+</sup>) solution (138 U), centrifuged, washed with the same buffer and centrifuged.

The carbon nanotubes modified with NAD<sup>+</sup> dependent glucose dehydrogenase obtained using the described strategies were then employed to modify the glassy carbon electrode.

### **2.3. Electrochemical instrumentation and electrode modification procedures**

Cyclic voltammetry experiments were performed using a CHI 700B bipotentiostat in a three-electrode arrangement with a calomel reference electrode (SCE) and a platinum sheet as the counter electrode. The GCEs were covered with a suspension of pristine SWCNTs (90 μl of suspension prepared from 8 mg of SWCNTs and 12 ml of ethanol) and next with 60 μl of modified SWCNTs suspension described above unless stated elsewhere. All current densities

were calculated using geometrical area of the GCE (BAS) ( $A = 0.071 \text{ cm}^2$ ). The biofuel cell parameters were examined in dioxygen saturated 0.2 M phosphate buffer solution, pH 6.0, which is a compromise between the pH values of maximum activity for both enzymes.

### 3. Results and discussion

#### 3.1 Oxygen electroreduction on SWCNT-covered electrodes in the presence and absence of fluorinated compounds

The aim of the preliminary experiments was to check whether perfluorodecalin film has the ability to increase the concentration of oxygen in the vicinity of the electrode and leads to higher oxygen reduction currents (Fig. 3).

Two GCE electrodes were used, one was covered by casting 30  $\mu\text{l}$ . of perfluorodecalin. Other two electrodes were modified as follows: first they were covered with a suspension of SWCNTs prepared by mixing 8 mg of nanotubes with 12 ml of 99.8% ethanol; then, following drying in air, 30  $\mu\text{l}$  of perfluorodecalin was casted on one of them and left to dry. Using each of these four electrodes, cyclic voltammograms were recorded in a solution containing McIlvaine buffer, pH = 5.3 saturated with oxygen.

Insert Fig. 3.

In the presence of precleaned pristine SWCNTs the oxygen reduction current appears at a potential less negative by ca. -0.3 V than that observed using bare GCE. Perfluorodecalin only slightly influences the potential, however, it stabilizes and accumulates oxygen and increases the oxygen reduction current indicating higher concentration of oxygen in the film compared to the aqueous solution. This is seen when bare GCE is used but and even more for the electrodes nanostructured with pristine carbon nanotubes. This is not unexpected since

solubility and effective diffusivity of oxygen in the hydrophobic fluorinated medium are reported to be larger than in the corresponding hydrocarbon or in aqueous solutions [58-60].

### **3.2 Laccase catalyzed oxygen reduction at electrodes modified with arylated SWCNTs in the presence and absence of perfluorodecalin**

The oxygen enrichment of the electrode surface achieved by the application of perfluorodecalin lead us to employ this compound in the reduction of oxygen catalyzed by laccase. The biocathode based on laccase and naphthylated carbon nanotubes described in our recent papers [35,36] were employed. Two SWCNTs nanostructured electrodes were immersed in the laccase solution (2.3 mg laccase in 2 ml McIlvaine buffer, pH = 5.3) and left overnight in the fridge. Next day one of the electrodes was covered by casting 30  $\mu$ l of perfluorodecalin. The onset of current of the catalytic curves is ca. 0.6V vs. SCE which is close to the formal potential of oxygen reduction at this pH: + 0.771V. At the perfluorodecalin covered electrode the current is almost twice larger (Fig. 4).

Insert Fig. 4.

### **3.3 Oxygen reduction at electrodes with SWCNTs modified with perfluoroaryl groups**

In order to simplify the procedure, we modified the carbon nanotubes with perfluoroaryl groups instead of the aryl. Fig. 3-C exhibits the large increase of current observed for electrodes modified with side perfluorophenylated nanotubes (material 3) without laccase which confirms enrichment of the environment with oxygen.

To study the effect of perfluorination on the catalytic currents in the presence of laccase, 8 electrodes were prepared by casting 90  $\mu$ l of the suspensions of all nanotubes studied (8 mg of modified SWCNTs in 12 ml ethanol) and cyclic voltammograms were recorded in the

deaerated and oxygenated buffer solutions. Next, the electrodes were immersed into laccase solution for a night and recording was repeated [Fig. 5].

Insert Fig. 5

Further improvement of current could be observed when the amount of SWCNTs at the electrode surface was increased to 100  $\mu\text{g}$  and the results can be seen in Fig. 6 both for the side and end (and defects) modified nanotubes.

Insert Fig. 6

### **3.4. Monitoring oxygen levels using side electrodes modified with side - perfluorophenylated SWCNTs (material 3) and laccase**

The GCE modified with 100  $\mu\text{g}$  of side - perfluorophenylated SWCNTs and adsorbed laccase were used for monitoring oxygenation of solution of McIlvaine buffer,  $\text{pH} = 5.3$ . Solutions were prepared by mixing oxygen saturated and deoxygenated buffer solution Fig. 7 shows the increase of current in the voltammetric experiment.

Insert Fig.7.

The plot of current measured at 0.2V vs. concentration of oxygen increases linearly up to about 0.6mM. At larger concentrations of oxygen in the solution the current still increases but slow leveling is observed.

### **3.5. Application of electrodes modified with perfluorophenylated SWCNTs and laccase in biofuel cell.**

Electrodes modified with perfluorophenylated SWCNTs and laccase were employed as biocathodes in a biofuel cell.  $\text{NAD}^+$  dependent GDH was used as the anode catalyst [35]. Fig. 8 demonstrates the binding scheme of GDH to the carbon nanotubes. The largest catalytic

current of glucose oxidation is obtained using aminoethylated SWCNTs bioconjugated to GDH (Fig. 8-B)

Insert Fig.8.

The biofuel cell composed of this electrode together with the cathode covered with side-perfluorophenylated SWCNTs and laccase gives the best output in terms of power as shown in Table 1. The open circuit potential of this cell is  $0.57\pm 0.05$  V and the maximum power density is  $0.865\pm 0.090$  mW/cm<sup>2</sup>.

Since the cofactor is not tightly bound in the enzyme either addition of soluble NAD<sup>+</sup> to the solution (Fig.8-A and B) or co-binding of the cofactor on the electrode (Fig.8-C) are required. The approach involving NAD<sup>+</sup> bonded to the SWCNTs was used for the biofuel cell shown in Fig. 9. Fig. 9A depicts the plots of power density and current density vs. cell voltage for this version of the fuel cell. Fig 9B shows the power – time dependence under external resistance of 1 MΩ.

Insert Fig. 9.

Insert Table 2.

#### **4. Conclusions**

Perfluorodecalin film but even more perfluorophenylated carbon nanotube network allows to achieve larger oxygen reduction currents. Perfluorocarbons with carbon skeletons saturated with fluorine are extremely hydrophobic and nonpolar which leads to increased oxygen solubility and effective diffusivity [60]. The effective oxygen diffusivities are 2.5 to 4-fold that of water or physiological salt solution. These desirable properties lead to several





important applications e.g. in oxygen delivery systems and blood substitutes. Kinetics of oxygen dissolution in fluorinated media has been also reported to be faster than in the corresponding hydrocarbons or aqueous solutions.[58,59] Nonpolar environment guides oxygen in proximity of the active site of the enzyme. The largest laccase catalyzed oxygen reduction currents are obtained using side-perfluorophenylated SWCNTs on the cathode. It should be underlined that the cathode process is direct electron transfer and no mediator is needed to obtain these large catalytic reduction currents. The degree of SWCNTs modification is larger for wall-modified nanotubes than in case of end modification and the length of the substituent is appropriate for direct electron transfer to the copper TI site. For carbon nanotube covered electrode in the absence of laccase, the reduction proceeds at -0.3V vs. SCE, while with laccase adsorbed by means of perfluorophenylated groups direct electron transfer takes place close to +0.6V. Maximum current and power density has been obtained for the glucose/oxygen fuel cell based on aminoethylated SWCNTs bioconjugated to GDH at the anode side and cathode covered with side - perfluorophenylated SWCNTs and laccase. The open circuit potential of this cell is  $0.57\pm 0.05$  V and the maximum power density is  $0.86\pm 0.09$  mW/cm<sup>2</sup>. This approach requires however addition of NAD<sup>+</sup> to the solution. Therefore, in this paper we also propose binding of NAD<sup>+</sup> to the carbon nanotubes (material C) which allows to eliminate the addition of this cofactor to the solution. The power output of such cell is still  $0.23\pm 0.03$  mW/cm<sup>2</sup> and the open circuit potential is  $0.65\pm 0.08$  V. The latter approach is important for the applications of biofuel cells in the biological media.

## Acknowledgements



This work was supported by Polish Ministry of Sciences and Higher Education No. N N204 214639 and grant PSPB 079/2010 from Switzerland through the Swiss Contribution to the enlarged European Union. Technical assistance by Paulina Nieścior is kindly acknowledged.

---

## References

- [1] A. Heller, Miniature biofuel cells, *Phys. Chem. Chem. Phys.* 6 (2004) 209.
- [2] S.C. Barton, J. Gallaway, P. Atanassov, Enzymatic biofuel cells for implantable and microscale devices, *Chem. Rev.* 104 (2004) 4867.
- [3] G.T.R. Palmore, H.H. Kim, Electro-enzymatic reduction of dioxygen to water in the cathode compartment of a biofuel cell, *J. Electroanal. Chem.* 464 (1999) 110.
- [4] J.A. Cracknell, K.A. Vincent, F.A. Armstrong, Enzymes as working or inspirational electrocatalysts for fuel cells and electrolysis, *Chem. Rev.* 108 (2008) 2439.
- [5] I. Willner, Y.M. Yan, B. Willner, R. Tel-Vered, Integrated Enzyme-Based Biofuel Cells—A Review, *Fuel Cells* 9 (2009) 7.
- [6] M.J. Cooney, V. Svoboda, C. Lau, G. Martin, S.D. Minteer, Enzyme catalysed biofuel cells *Energy Environ. Sci.* 1 (2008) 320.
- [7] E. Nazaruk, S. Smoliński, M. Swatko-Ossor, G. Ginalska, J. Fiedurek, J. Rogalski, R. Bilewicz, Enzymatic biofuel cell based on electrodes modified with lipid liquid-crystalline cubic phase. *J. Power Sources* 183 (2008) 533.

[8] P. Cinquin, Ch. Gondran, F. Giroud, S. Mazabrard, A. Pellissier, F. Boucher, J.P. Alcaraz, K. Gorgy, F. Lenouvel, S. Mathe, P. Porcu, S. Cosnier, A glucose biofuel cell implanted in rats. *Plos One* 5 (2010) 10476.

[9] R. Bilewicz, M. Opallo, *Fuel Cell Science: theory, fundamentals and biocatalysis*, Andrzej Wieckowski, Editor, John Wiley & Sons, Inc, Hoboken, New Jersey, 2010, p 169

[10] T. Tamaki, Enzymatic Biofuel Cells Based on Three-Dimensional Conducting Electrode Matrices, *Top. Catal.* 55 (2012) 1162.

[11] I. Ivanov, Vidakovic T. Koch, K. Sundmacher, Recent Advances in Enzymatic Fuel Cells: Experiments and Modeling, *Energies* 3 (2010) 803.

[12] M. Falk, Z. Blum, S. Shleev, Direct electron transfer based enzymatic fuel cells, *Electrochim. Acta* 82 (2012) 191.

[13] A. Zebda, C. Gondran, A. Le Goff, M. Holzinger, P. Cinquin, S. Cosnier, Mediatorless high-power glucose biofuel cells based on compressed carbon nanotube-enzyme electrodes, *Nat. Commun.* 2 (2011) 370.

[14] Sakai, H. Nakagawa, T. Tokita, Y. Hatazawa, T. Ikeda, T. Tsjimura, S. Kano, K. A high-power glucose/oxygen biofuel cell operating under quiescent conditions, *Energy Environ. Sci.* 2 (2009) 133.

[15] R.L. Arechederra, S.D. Minter, Complete oxidation of glycerol in an enzymatic biofuel cell, *Fuel Cells* 9 (2009) 63.

[16] Treu, B.L. Arechederra, R.L. Minter, S.D. Bioelectrocatalysis of Ethanol via PQQ-Dependent Dehydrogenases Utilizing Carbon Nanomaterial Supports, *J. Nanosci. Nanotechnol.* 9 (2009) 2374.



- [17] Tasca, F. Gorton, L. Harreither, W. Haltrich, D. Ludwig, R. Noll, G. Comparison of direct and mediated electron transfer for cellobiose dehydrogenase from *Phanerochaete sordida*, *Anal. Chem.* 81 (2009) 2791.
- [18] M. Sosna, L. Stoica, E. Wright, J.D. Kilburn, W. Schuhmann, P.N. Bartlett, Mass transport controlled oxygen reduction at anthraquinone modified 3D-CNT electrodes with immobilized *Trametes hirsuta* laccase. *Phys. Chem. Chem. Phys.* 14 (2012) 11882.
- [19] A. Zloczewska, M. Jonsson-Niedziolka, J. Rogalski, M. Opallo, Vertically aligned carbon nanotube film electrodes for bioelectrocatalytic dioxygen reduction, *Electrochim. Acta* 56 (2011) 3947.
- [20] F. Gao, L. Viry, M. Maugey, P. Poulin, N. Mano, Engineering hybrid nanotube wires for high-power biofuel cells, *Nat. Commun.* 2 (2010) 370.
- [21] T. Miyake, S. Yoshino, T. Yamada, K. Hata, M. Nishizawa, Self-Regulating Enzyme–Nanotube Ensemble Films and Their Application as Flexible Electrodes for Biofuel Cells, *J. Am. Chem. Soc.* 133 (2011) 5129.
- [22] A. Zebda, C. Gondran, P. Cinquin, S. Cosnier, Glucose biofuel cell construction based on enzyme, graphite particle and redox mediator compression, *Sens. Actuators, B* 173 (2012) 760.
- [23] S.C. Barton, Oxygen Transport in Composite Mediated Biocathodes, *Electrochim. Acta* 50 (2005) 2145.
- [24] N.S. Hudak, J.W. Gallaway, S.C. Barton, Formation of mediated biocatalytic cathodes by electrodeposition of a redox polymer and laccase, *J. Electrochem. Soc.* 629 (2009) 57.
- [25] L. Brunel, J. Denele, K. Servat, K.B. Kokoh, C. Jolival, C. Innocent, M. Cretin, M. Rolland, S. Tingry, Oxygen transport through laccase biocathodes for a membrane-less glucose/O<sub>2</sub> biofuel cell, *Electrochem. Commun.* 9 (2007) 331.



- [26] G. Gupta, C. Lau, F. Rajendran, F. Colon, B. Branch, D. Ivnitski, P. Atanassov, Direct electron transfer catalyzed by bilirubin oxidase for air breathing gas-diffusion electrodes, *Electrochem. Commun.* 13 (2011) 247.
- [27] C. Lau, E.R. Adkins, R.P. Ramasamy, H.R. Luckarift, G.R. Johnson, P. Atanassov, Design of carbon nanotube-based gas-diffusion cathode for O<sub>2</sub> reduction by multicopper oxidases, *Adv. Energy Mater.* 2 (2012) 162.
- [28] G.P.M.K. Ciniciato, C. Lau, A. Cochrane, S.S. Sibbett, E.R. Gonzalez, P. Atanassov, Development of paper based electrodes: From air-breathing to paintable enzymatic cathodes, *Electrochim. Acta* 82 (2012) 208.
- [29] E. Nazaruk, K. Sadowska, K. Madrak, J.F. Biernat, J. Rogalski, R. Bilewicz, Composite bioelectrodes based on lipidic cubic phase with carbon nanotube network, *Electroanal.* 21 (2009) 507.
- [30] K. Sadowska, K. Stolarczyk, J.F. Biernat, K.P. Roberts, J. Rogalski, R. Bilewicz, Derivatization of single-walled carbon nanotubes with redox mediator for biocatalytic oxygen electrodes, *Bioelectrochem.* 80 (2010) 73.
- [31] E. Nazaruk, K. Sadowska, J.F. Biernat, J. Rogalski, G. Ginalska, R. Bilewicz, Enzymatic electrodes nanostructured with functionalized carbon nanotubes for biofuel cell applications, *Anal. Bioanal. Chem.* 398 (2010) 1651.
- [32] K. Stolarczyk, M. Sepelowska, D. Lyp, K. Zelechowska, J. F. Biernat, J. Rogalski, K. D. Farmer, K. P. Roberts, R. Bilewicz, Hybrid biobattery based on arylated carbon nanotubes and laccase, *Bioelectrochem.* 87 (2012) 154.
- [33] E. Nazaruk, M. Karaskiewicz, K. Żelechowska, J.F. Biernat, J. Rogalski, R. Bilewicz, Powerful connection of laccase and carbon nanotubes: Material for mediator-free electron transport on the enzymatic cathode of the biobattery, *Electrochem. Commun.* 14 (2012) 67.



- [34] M. Karaškiewicz, E. Nazaruk, K. Żelechowska, J.F. Biernat, J. Rogalski, R. Bilewicz, Fully enzymatic mediatorless fuel cell with efficient naphthylated carbon nanotube-laccase composite cathodes, *Electrochem. Commun.* 20 (2012) 124.
- [35] K. Stolarczyk, D. Lyp, K. Żelechowska, J.F. Biernat, J. Rogalski, R. Bilewicz, Arylated carbon nanotubes for biobatteries and biofuel cells, *Electrochim. Acta* 79 (2012) 74.
- [36] E. Nazaruk, E. Górecka, R. Bilewicz, Enzymes and mediators hosted together in lipidic mesophases for the construction of biodevices, *J. Colloids Interface Sci.* 385 (2012) 130.
- [37] K. Karnicka, K. Miecznikowski, B. Kowalewska, M. Skunik, M. Opallo, J. Rogalski, W. Schuhmann, P.J. Kulesza, ABTS-modified multi-walled carbon nanotubes as effective mediating system for bioelectrocatalytic reduction of oxygen, *Anal. Chem.* 80 (2008) 7643
- [38] F. Tasca, L. Gorton, M. Kujawa, I. Patel, W. Harreither, C.K. Peterbauer, R. Ludwig, G. Nöll, Increasing the coulombic efficiency of glucose biofuel cell anodes by combination of redox enzymes, *Biosens. Bioelectron.* 25 (2010) 1710.
- [39] M.T. Meredith, M. Minson, D. Hickey, K. Artyushkova, D.T. Glatzhofer, S.D. Minteer, Anthracene-Modified Multi-Walled Carbon Nanotubes as Direct Electron Transfer Scaffolds for Enzymatic Oxygen Reduction, *ACS Catalysis* 1 (2012) 1683.
- [40] G. Strack, R. Luckarift, S.R. Sizemore, R.K. Nichols, K.E. Farrington, P.K. Wu, P. Atanassov, J.C. Biffinger, G.R. Johnson, Power generation from a hybrid biological fuel cell in seawater, *Bioresource Technol.* 128 (2013) 222.
- [41] J. Filip, J. Šefčovičová, P. Gemeiner, J. Tkac, Electrochemistry of bilirubin oxidase and its use in preparation of a low cost enzymatic biofuel cell based on a renewable composite binder chitosan *Electrochim. Acta* 87 (2013) 366.



- [42] D. Leech, P. Kavanagh, W. Schuhmann, Enzymatic fuel cells: Recent progress, *Electrochim. Acta* 84 (2012) 223.
- [43] D. Long, G. Wu, G. Zhu, Noncovalently Modified Carbon Nanotubes with Carboxymethylated Chitosan: A Controllable Donor-Acceptor Nanohybrid *Int. J. Mol. Sci.* 9 (2008) 120.
- [44] W. Chiang, B.E. Brinson, A.Y. Huang, P.A. Willis, M.J. Bronikowski, J.L. Margrave, R.E. Smalley, R.H. Hauge, Purification and Characterization of Single-Wall Carbon Nanotubes (SWNTs) Obtained from the Gas-Phase Decomposition of CO (HiPco Process) *J. Phys. Chem. B* 105 (2001) 8297.
- [45] E.P. Dillon, C.A. Crouse, A.R. Barron, Synthesis, Characterization, and Carbon Dioxide Adsorption of Covalently Attached Polyethyleneimine-Functionalized Single-Wall Carbon Nanotubes, *ACS Nano*, 2 (2008) 156.
- [46] J. Zhang, H. Zou, Q. Qing, Y. Yang, Q. Li, Z. Liu, X. Guo, Z. Du, Effect of Chemical Oxidation on the Structure of Single-Walled Carbon Nanotubes, *J. Phys. Chem. B* 107 (2003) 3712.
- [47] A.R. Harutyunyan, B.K. Pradhan, J.P. Chang, G.G. Chen, P.C. Eklund, Purification of single-walled carbon nanotubes by selective microwave heating of catalyst particles, *J. Phys. Chem. B* 106 (2002) 8671.
- [48] T. Mugadza, T. Nyokong, Covalent linking of ethylene diamine functionalized single walled carbon nanotubes to cobalt (II) tetracarboxyl-phthalocyanines for use in electrocatalysis, *Synth. Met.* 160 (2010) 2089.
- [49] A. Hirsch, Functionalization of Single-Walled Carbon Nanotubes, *Angew. Chem. Int. Ed.* 41 (2002) 1853.



- [50] M.S. Dresselhaus, G. Dresselhaus, R. Saito, A. Jorio, Raman spectroscopy of carbon nanotubes, *Phys. Rep.* 409 (2005) 47.
- [51] C. Fantini, M.L. Usrey, M.S. Strano, Investigation of Electronic and Vibrational Properties of Single-Walled Carbon Nanotubes Functionalized with Diazonium Salts, *J. Phys. Chem. C* 111 (2007) 17941.
- [52] K. Sadowska, K.P. Roberts, R. Wisner, J.F. Biernat, E. Jabłowska, R. Bilewicz, Synthesis, characterization, and electrochemical testing of carbon nanotubes derivatized with azobenzene and anthraquinone, *Carbon* 47 (2009) 1501.
- [53] K. Sadowska, E. Jabłowska, K. Stolarczyk, R. Wisner, R. Bilewicz, K.P. Roberts, J.F. Biernat, Chemically modified carbon nanotubes: Synthesis and implementation, *Pol. J. Chem.* 82 (2008) 1309.
- [54] D.A. Lappi, F.E. Stolzenbach, N.O. Kaplan, M.D. Kamen, Immobilization of hydrogenase on glass beads, *Biochem. Biophys. Res. Commun.* 69 (1976) 878.
- [55] B.T. Kaufman, J.V. Pierce, Purification of dihydrofolate reductase from chicken liver by affinity chromatography, *Biochem. Biophys. Res. Commun.* 44 (1971) 608.
- [56] M. Landt, S.C. Boltz, L.G. Butler, *Biochemistry*, 1978, 17, 915; Scouten W.H., in: Elving P.J., Winefordner J.D. (eds.), *Affinity chromatography: Bioselective Adsorption on Inert Matrices*, John Wiley and Sons, New York, 1980, pp. 42-84
- [57] J. Rogalski, A. Dawidowicz, Controlled porous glass (CPG) with reactive epoxy groups as support for affinity chromatography. I. Optimization of CPG modification and the binding of glucose with modified surface, *Acta Biotechnol.* 9 (1989) 275.
- [58] A.M.A. Dias, R.P. Banifácio, I.M. Marrucho, A.A.H. Pádua, M.F. Costa Gomes, Solubility of oxygen in *n*-hexane and in *n*-perfluorohexane. Experimental determination and prediction by molecular simulation, *Chem. Phys. Phys. Chem.* 5 (2003) 543.



[59] A.M.A. Dias, C.M.B. Gonçalves, J.L. Legido, J.A.P. Coutinho, I.M. Marrucho, Solubility of oxygen in substituted perfluorocarbons, *Fluid Phase Equilibria* 238 (2005) 7.

[60] C.A. Fraker, A.J. Mendez, C.L. Stabler, Complementary methods for the determination of dissolved oxygen content in perfluorocarbon emulsions and other solutions, *J. Phys.Chem., B*, 115 (2011)10547.

## Figure Captions:

Figure 1. Examples of Raman spectra of described modified carbon nanotubes.

Figure 2. Examples of TGA analyses

Fig. 3 Cyclic voltammograms recorded in (—) oxygenated (—) deoxygenated McIlvaine buffer, pH = 5.3 using GCE (A1 and A2) and GCE covered with SWCNTs (B1 and B2) without (A1 and B1) and with (A2 and B2) perfluorodecalin; (C) GCE covered with 60  $\mu\text{g}$  side perfluorophenylated SWCNTs (material 3);  $v =$  (A1, A2) 100 mV/s and (B1, B2, C) 5 mV/s.

Fig. 4. Cyclic voltammograms recorded in (—)deoxygenated, and (— and —) oxygenated McIlvaine buffer, pH = 5.3 using GCE with 60  $\mu\text{g}$  of naphtylated SWCNTs (inset) and laccase, (—) same electrode but with a perfluorodecalin film;  $v = 1$  mV/s.

Fig. 5. Cyclic voltammograms recorded in (—)deoxygenated, and (— ) oxygenated McIlvaine buffer, pH = 5.3 using GCE with 60  $\mu\text{g}$  (B) phenylated and (A,C,D) perfluorophenylated SWCNTs and laccase,  $v = 1$  mV/s.

Fig. 6. Cyclic voltammograms recorded in (—)deoxygenated, and (— ) oxygenated McIlvaine buffer, pH = 5.3 using GCE with 100  $\mu\text{g}$  of SWCNTs (A) material 3, and (B) material 7 and laccase,;  $v = 1$  mV/s.

Fig. 7. Application of GCE modified with 100  $\mu\text{g}$  of perfluorophenylated SWCNTs (material 3) and laccase for monitoring oxygen in McIlvaine buffer solution, pH = 5.3. (A) voltammetric curves for increasing levels of oxygen in the solution. (B) plot of current at 0.2V vs. oxygen concentration.

Fig. 8. Binding schemes of GDH and cyclic voltammetry curves of catalytic glucose oxidation. Solution: McIlvaine buffer, pH = 6 containing (black line) 0, and (red line) 100 mM glucose and  $\text{NAD}^+$  : (A,B) 5 and (C) 0 mM.  $v = 1 \text{ mV/s}$ .

Fig. 9. Biofuel cell power plot (A) for bioconjugate C with bound  $\text{NAD}^+$  at the anode and SWCNTs (Material 3) and laccase at the cathode in oxygen saturated McIlvaine buffer solution, pH 6.0 containing 100 mM glucose. (B) Changes of current with time under  $1 \text{ M}\Omega$  external resistance.

Scheme 1. Syntheses of derivatized SWCNT.

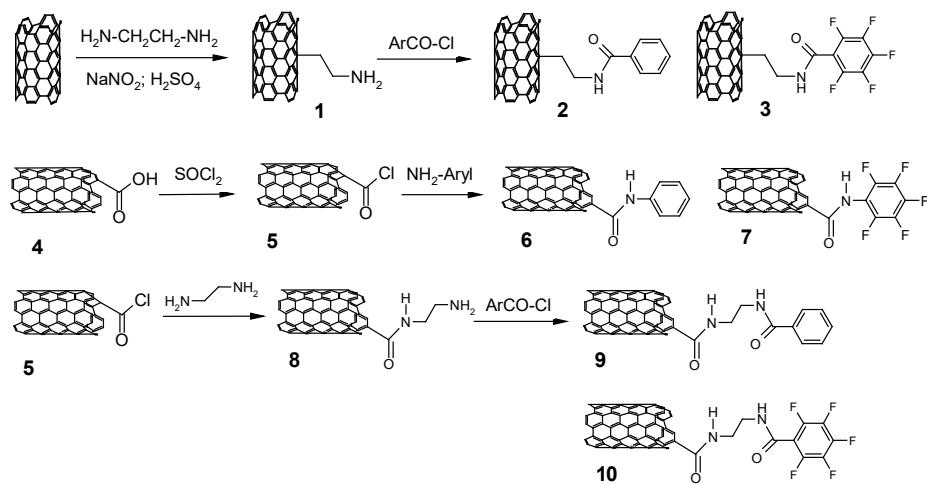


Table 1. Thermogravimetry and Raman characterization of modified SWCNTs.

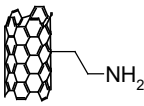
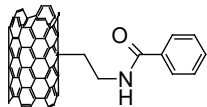
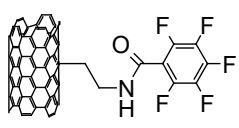
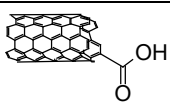
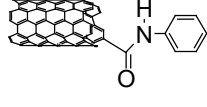
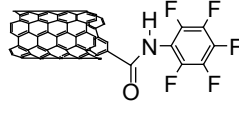
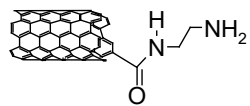
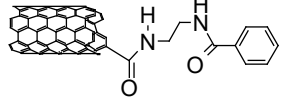
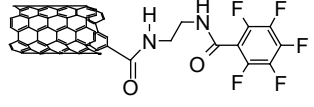
No of material and schematic formula	Derivatization degree, TGA up to 600°C Max DTG	Raman spectroscopy		
		D/G	G'/G	G'/D
 <b>1</b>	$0.082/7.9=1.0 \times 10^{-2}$	0.055	0.409	7.472
 <b>2</b>	$0.114/7 = 1.6 \times 10^{-2}$ Max 65, 158°C	0.094	0.312	3.331
 <b>3</b>	$0.063/7 = 0.9 \times 10^{-2}$ $0.063/6.9 = 0.9 \times 10^{-2}$ Max 155, 320°C	0.099	0.319	3.220
 <b>4</b>	$0.2/6.5=3.1 \times 10^{-2}$	0.091	0.291	3.195
 <b>6</b>	$0.132/6.83 = 2 \times 10^{-2}$	0.143	0.302	2.109
 <b>7</b>	$0.053/7.25 = 7.3 \times 10^{-3}$ Max 136°C	0.098	0.316	3.217
 <b>8</b>	$0.1/7=1.4 \times 10^{-2}$	0.055	0.404	7.296
 <b>9</b>	$0.078/6 = 1.3 \times 10^{-2}$ Max 118 i 305	0.138	0.286	2.077
 <b>10</b>	$0.05/6.75 - 7.4 \times 10^{-3}$ Max 189°C	0.134	0.298	2.222



Table 2. Parameters of the biofuel cells based on perfluorophenylated SWCNTs and laccase on the cathode and GDH bioconjugates on the anode.

GCE modification material (anode)	GCE modification material (cathode)	OCV (V)	max. power density ( $\mu\text{Wcm}^{-2}$ )	current of max. power density ( $\text{mAcm}^{-2}$ )	potential of max. power density (V)
A	3	0.58±0.06	678±50	3.11±0.12	0.22±0.02
	6	0.58±0.07	448±46	1.78±0.05	0.25±0.03
	7	0.56±0.06	576±61	2.85±0.09	0.20±0.02
	10	0.60±0.08	574±50	2.85±0.10	0.20±0.03
B	3	0.57±0.05	865±90	3.52±0.20	0.25±0.03
	6	0.57±0.07	503±65	1.89±0.06	0.18±0.02
	7	0.55±0.06	734±70	3.24±0.19	0.22±0.03
	10	0.58±0.08	663±50	3.08±0.15	0.22±0.03
C	3	0.65±0.08	226±31	0.56±0.02	0.39±0.05
	6	0.65±0.07	180±22	0.49±0.06	0.37±0.04
	7	0.64±0.05	198±29	0.54±0.09	0.37±0.06
	10	0.66±0.06	190±35	0.50±0.07	0.38±0.03

Figure 1. Examples of Raman spectra of described modified carbon nanotubes.

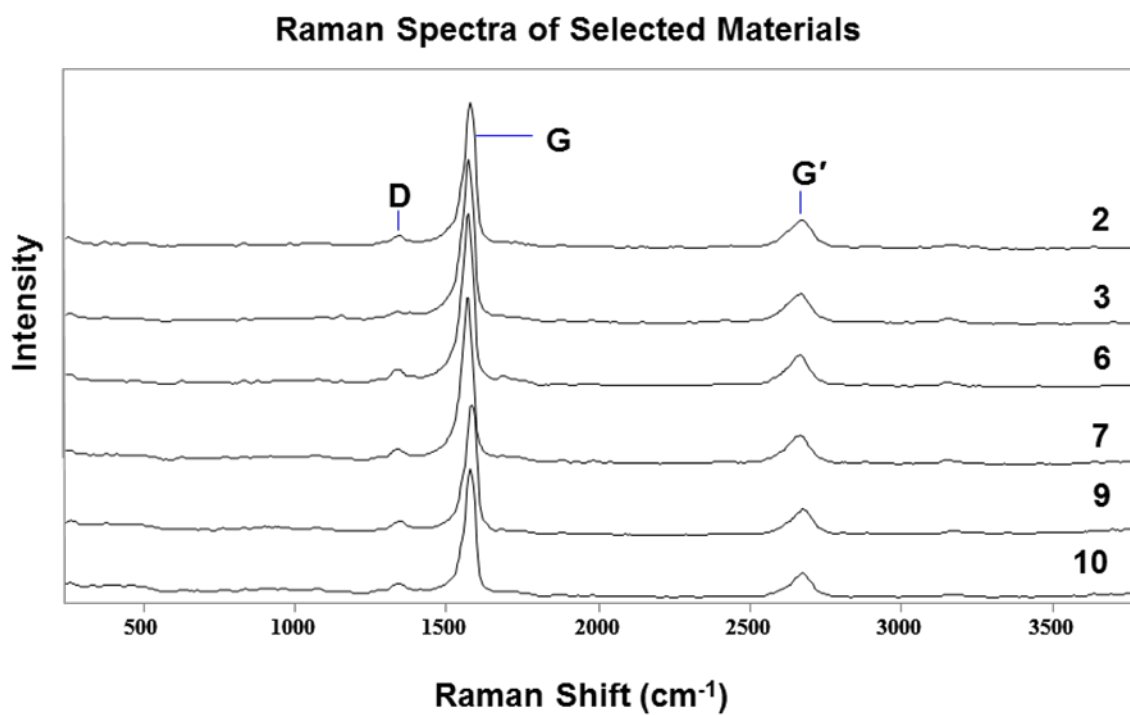


Figure 2. Examples of TGA analyses

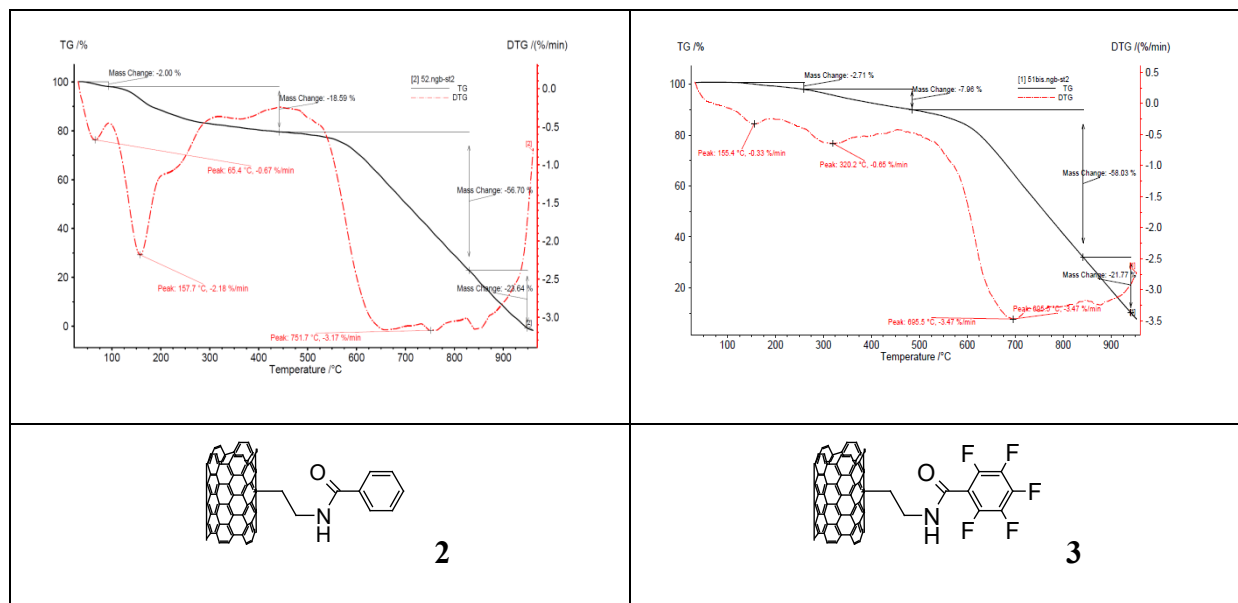




Fig. 3 Cyclic voltammograms recorded in (—) oxygenated (—) deoxygenated McIlvaine buffer, pH = 5.3 using GCE (A1 and A2) and GCE covered with SWCNTs (B1 and B2) without (A1 and B1) and with (A2 and B2) perfluorodecalin; (C) GCE covered with 60  $\mu\text{g}$  side perfluorophenylated SWCNTs (material 3);  $v =$  (A1, A2) 100 mV/s and (B1, B2, C) 5 mV/s.

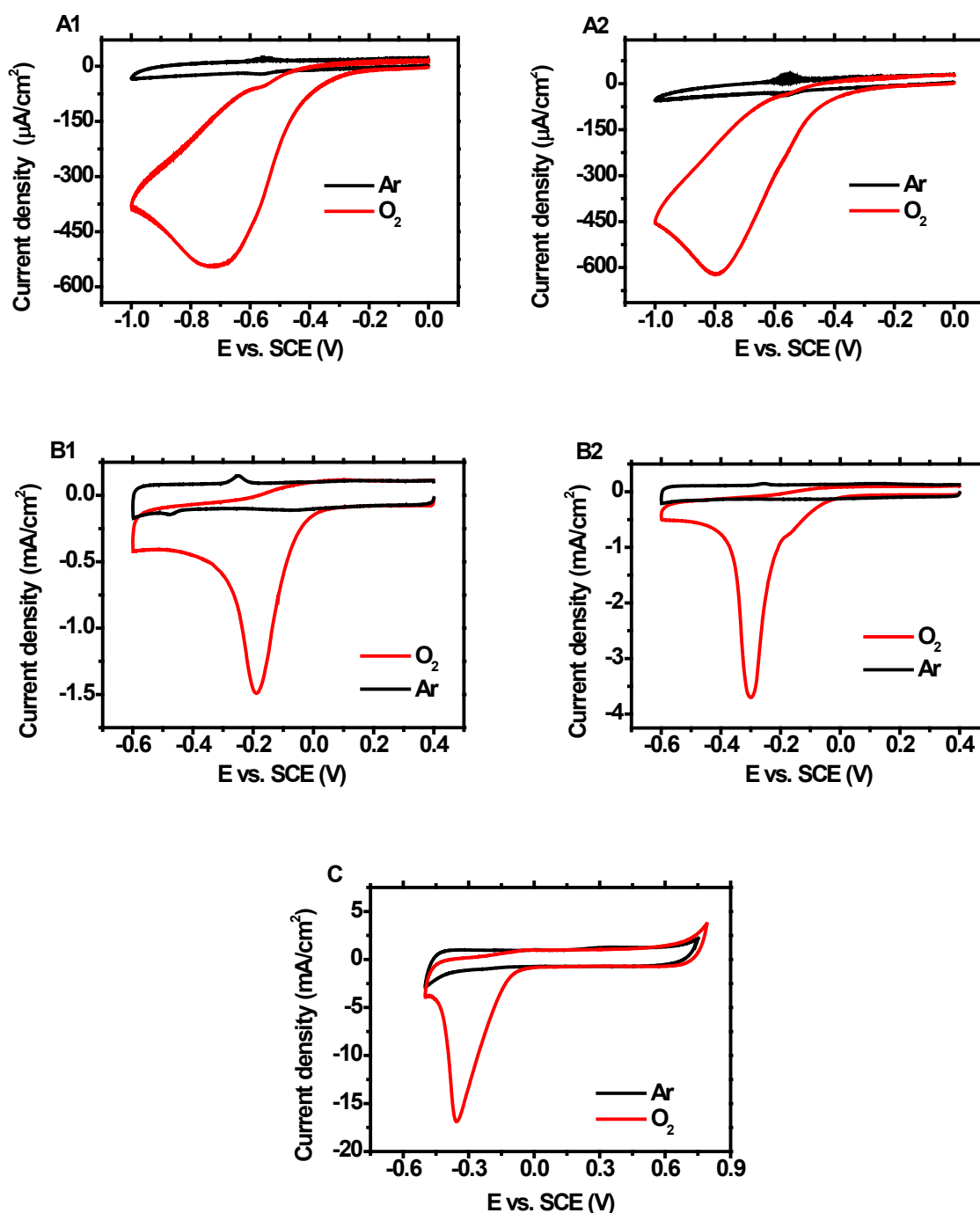


Fig. 4. Cyclic voltammograms recorded in (—)deoxygenated, and (— and —) oxygenated McIlvaine buffer, pH = 5.3 using GCE with 60  $\mu\text{g}$  of naphthylated SWCNTs (inset) and laccase, (—) same electrode but with a perfluorodecalin film;  $v = 1 \text{ mV/s}$ .

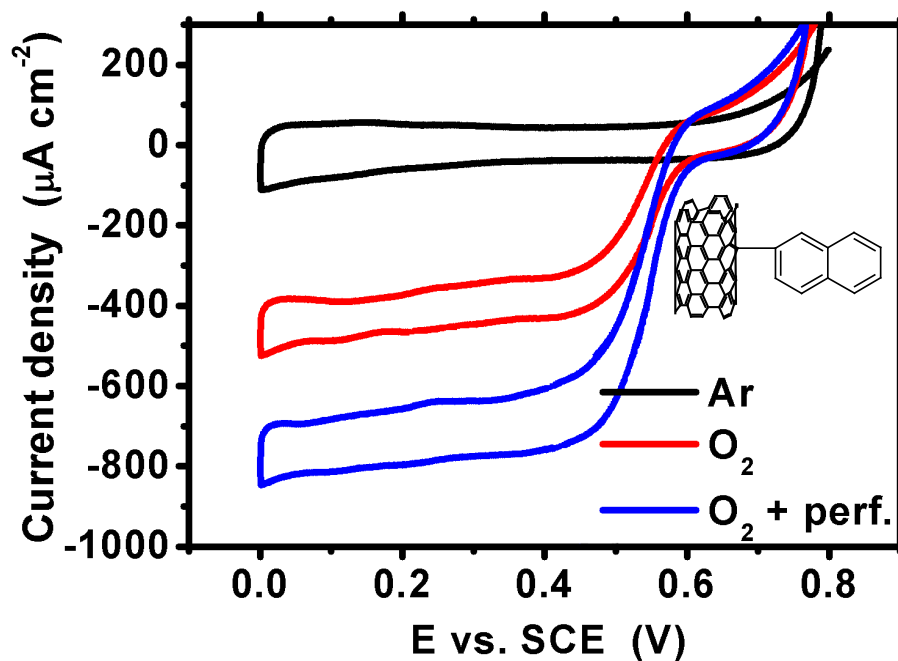


Fig. 5. Cyclic voltammograms recorded in (—)deoxygenated, and (—) oxygenated McIlvaine buffer, pH = 5.3 using GCE with 60  $\mu\text{g}$  (B) phenylated and (A,C,D) perfluorophenylated SWCNTs and laccase,  $v = 1 \text{ mV/s}$ .



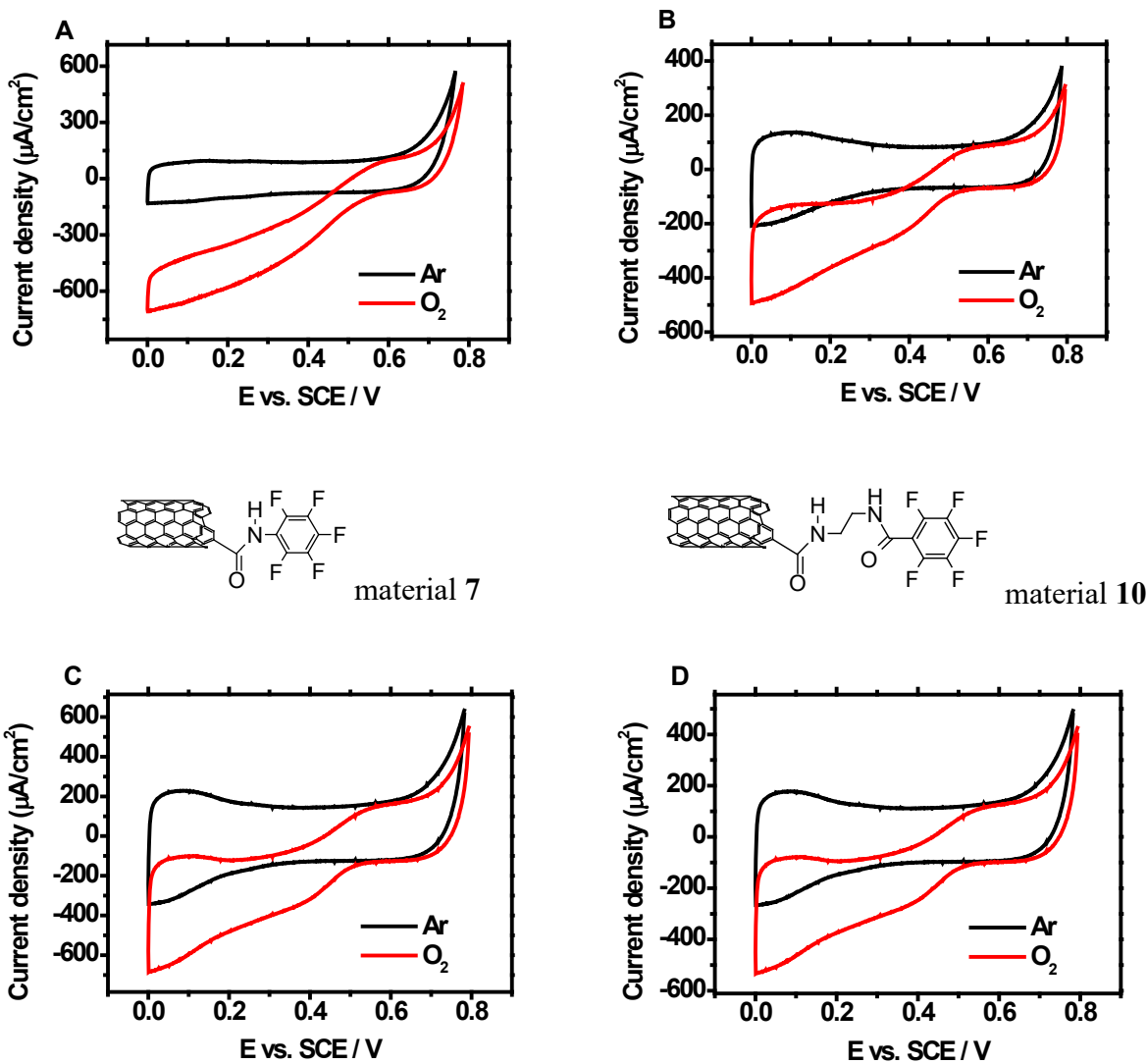


Fig. 6. Cyclic voltammograms recorded in (—)deoxygenated, and (—) oxygenated McIlvaine buffer, pH = 5.3 using GCE with 100  $\mu\text{g}$  of SWCNTs (A) material 3, and (B) material 7 and laccase,;  $v = 1 \text{ mV/s}$ .



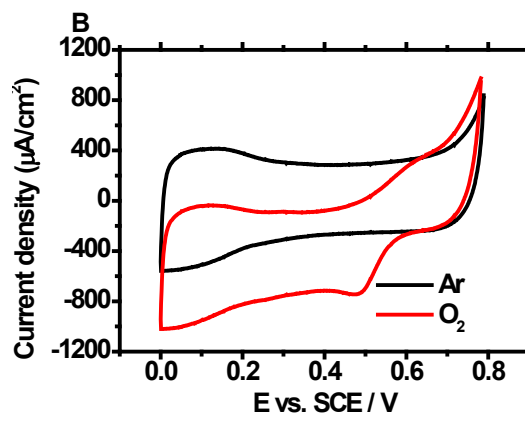
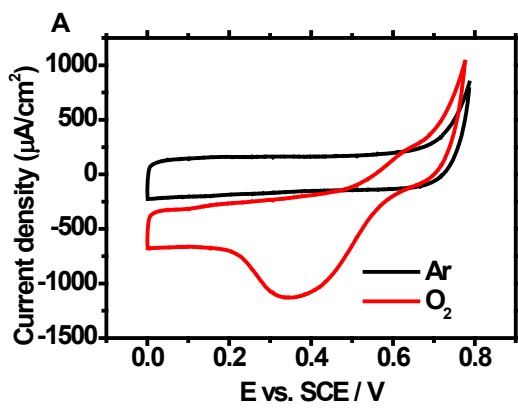


Fig. 7. Application of GCE modified with 100  $\mu\text{g}$  of perfluorophenylated SWCNTs (material 3) and laccase for monitoring oxygen in McIlvaine buffer solution,  $\text{pH} = 5.3$ . (A) voltammetric curves for increasing levels of oxygen in the solution. (B) plot of current at 0.2V vs. oxygen concentration.

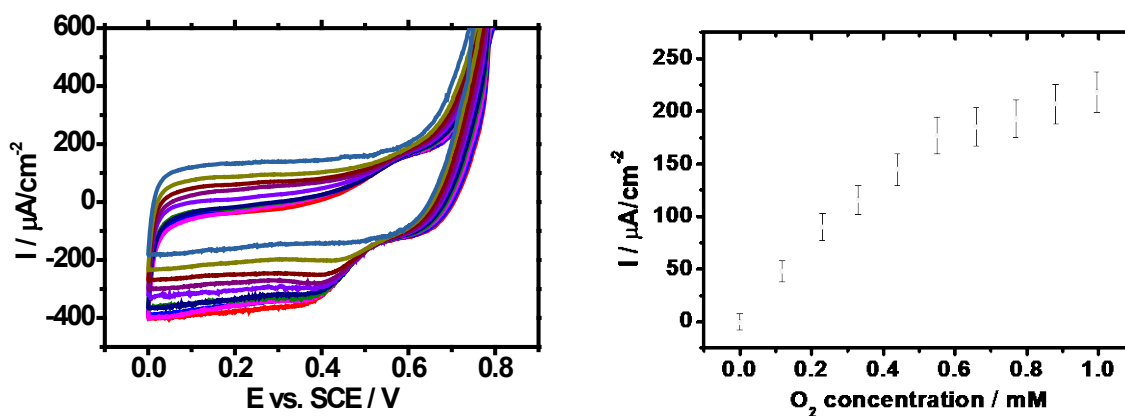


Fig. 8. Binding schemes of GDH and cyclic voltammetry curves of catalytic glucose oxidation. Solution: McIlvaine buffer, pH = 6 containing (black line) 0, and (red line) 100 mM glucose and  $\text{NAD}^+$  : (A,B) 5 and (C) 0 mM.  $v = 1 \text{ mV/s}$ .

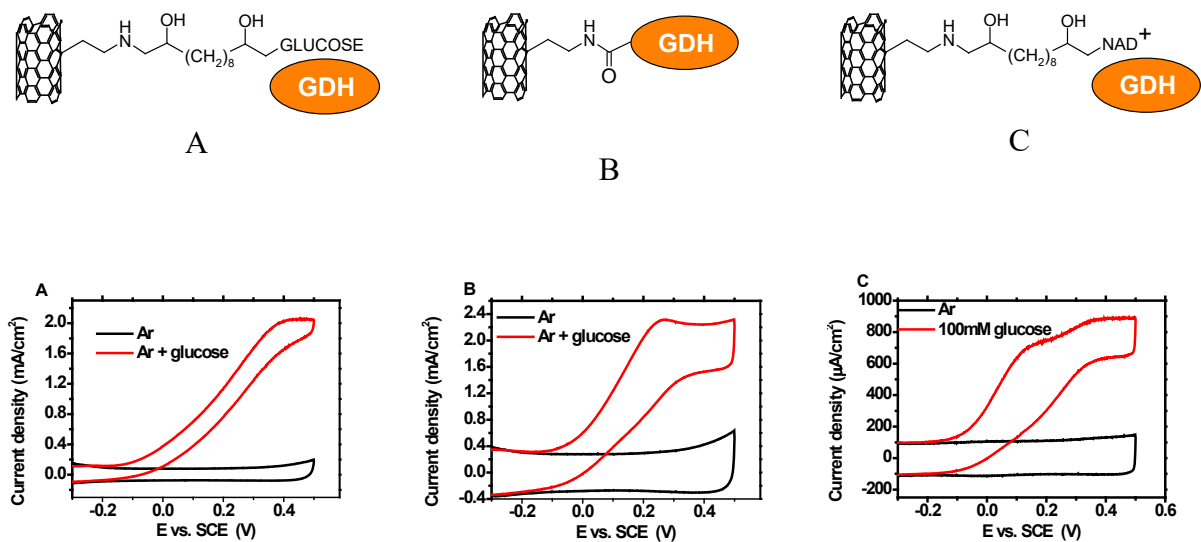


Fig. 9. Biofuel cell power plot (A) for bioconjugate C with bound  $\text{NAD}^+$  at the anode and SWCNTs (Material 3) and laccase at the cathode in oxygen saturated McIlvaine buffer solution, pH 6.0 containing 100 mM glucose. (B) Changes of current with time under 1  $\text{M}\Omega$  external resistance.

